Supporting information

Highly selective sensing of Fe^{3+} by an anionic metal−organic framework containing uncoordinated nitrogen and carboxylate oxygen sites

Chun-Hui Chen, [#a, b] Xu-Sheng Wang, [#b, c] Lan Li, [b] Yuan-Biao Huang [b*] & Rong Cao [a, b, c*]

[a] Department of Chemistry, University of Science and Technology of China, Hefei, Anhui 230026, P. R. China.

[b] State Key Laboratory of Structural Chemistry, Fujian Institute of Research on the Structure of Matter, Chinese Academy of Sciences, Fuzhou, Fujian, 350002, China.

[c] University of the Chinese Academy of Sciences, Beijing, 100049, China.

[#] C.-H. Chen and X.-S. Wang contributed equally to this work.

1. Crystal description of FJI-C8

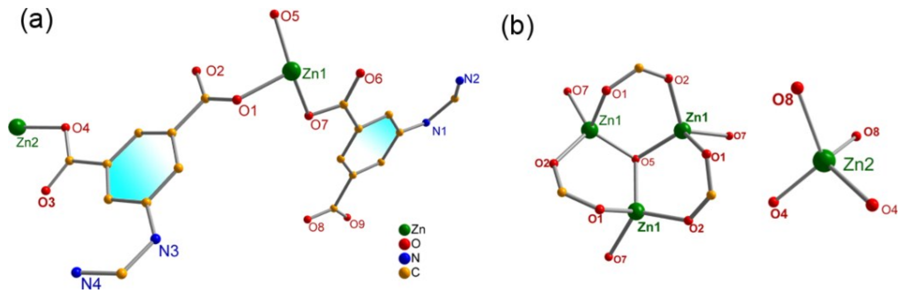

Fig. S1 (a) The coordination environment of ligand $\mathbf{H_6L}$; (b) The coordination environment of Zn_3O cluster and mono-zinc ion.

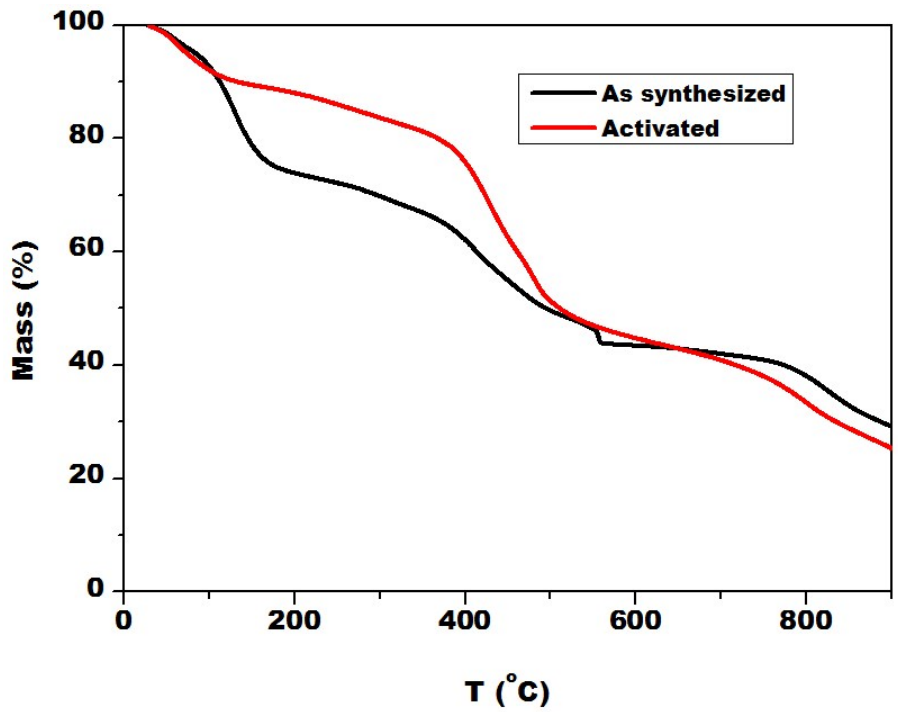

Fig. S2 TG of as synthesized and activated **FJI-C8**

The loss of guest molecules and $Me_2NH_2^+$ cations were started from room temperature to 400 ^oC concurrently. Then the structure compound starts to decompose.

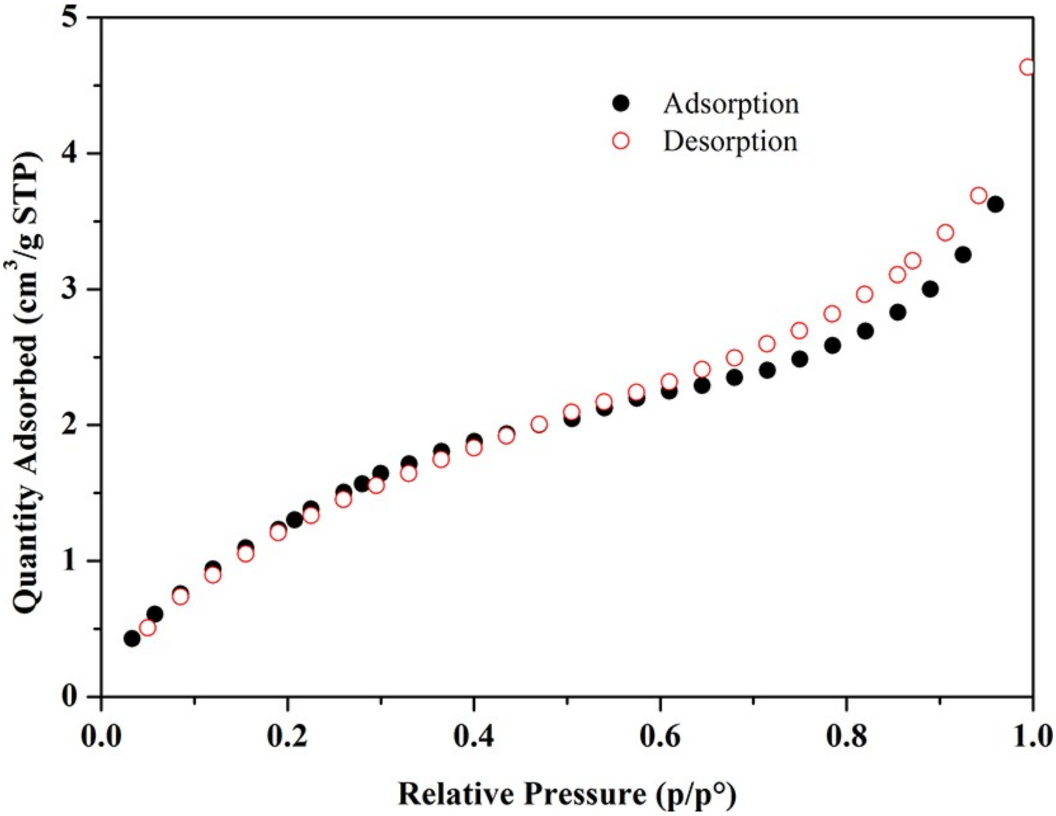

Fig. S3 The N_2 sorption of **FJI-C8**.

2. Ions detection with FJI-C8 suspension

Table S1 Quenching effect coefficients (K_{sv}) of different metal ions detected by **FJI-C8** suspension sample.

No.	Metal ion	K_{sv} (M^{-1})
1	Sr^{2+}	176
2	Na^{+}	177
3	Ca^{2+}	212
4	Gd^{3+}	255
5	Zn^{2+}	260
6	Al^{3+}	336
7	Cd^{2+}	345
8	Mn^{2+}	400
9	Bi^{3+}	426
10	Ni^{2+}	435
11	K^{+}	667
12	Mg^{2+}	886
13	Co^{2+}	1205
14	Cr^{3+}	1224
15	Cu^{2+}	2241
16	Fe^{3+}	8245

Table S2 Quenching effect coefficients (K_{sv}) of different anions detected by **FJI-C8** suspension sample.

No.	Anions	K_{sv} (M^{-1})
1	NO_3^{-}	177
2	Br^{-}	194
3	ClO_4^{-}	243
4	F^{-}	300
5	I^{-}	347
6	NO_2^{-}	356

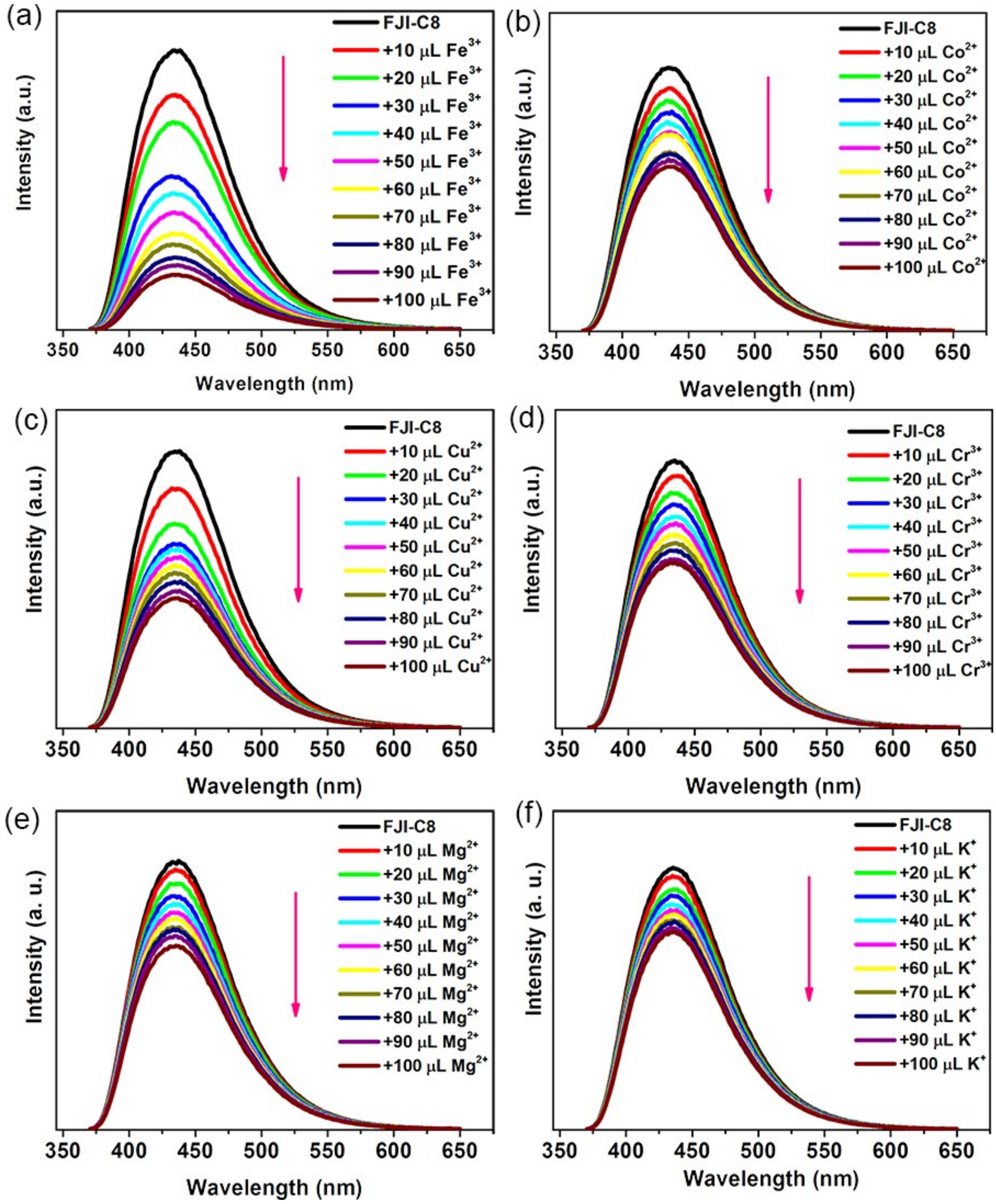

Fig. S4 Fluorescence spectra of **FJI-C8** suspended in DMF (2 mg/mL) upon incremental addition of $M(NO_3)_x$ (10 mM).

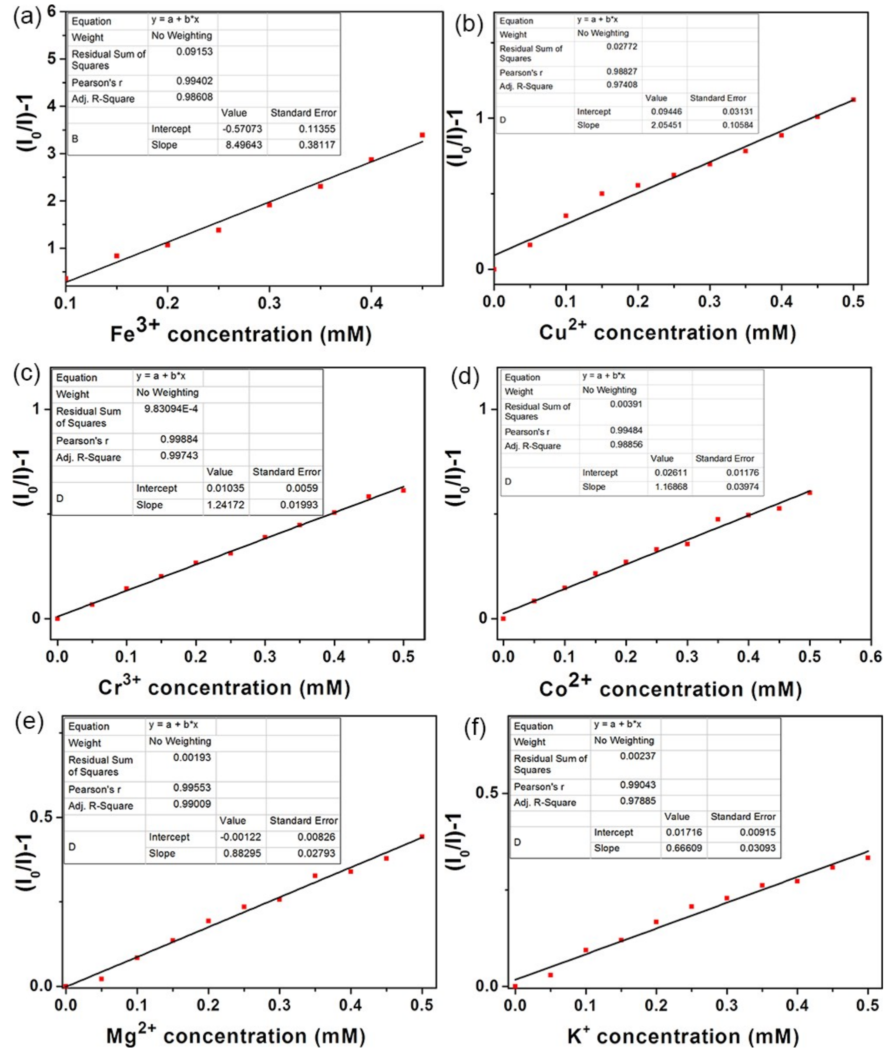

Fig. S5 S-V plot of **FJI-C8** suspended in DMF (2 mg/mL) upon incremental addition of $M(NO_3)_x$ (10 mM).

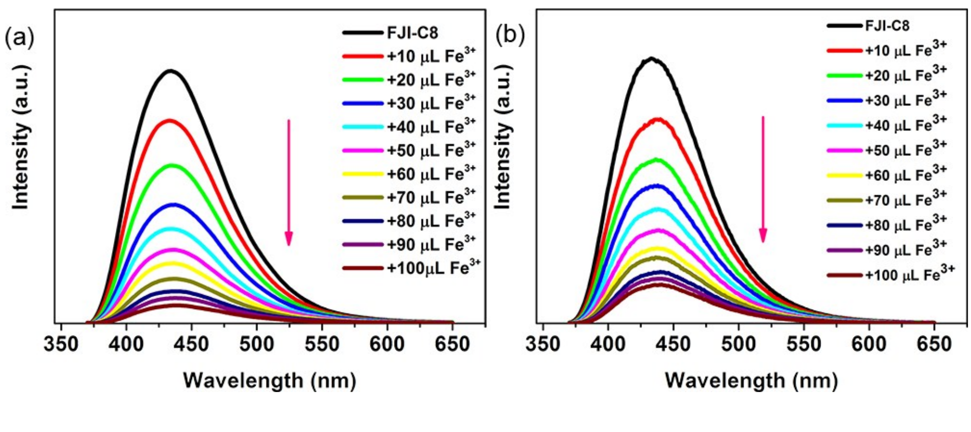

Fig. S6 Fluorescence spectra of **FJI-C8** suspended in DMF (a) 0.4 mg/mL, (b) 0.04 mg/mL upon incremental addition of $M(NO_3)_x$ (10 mM).

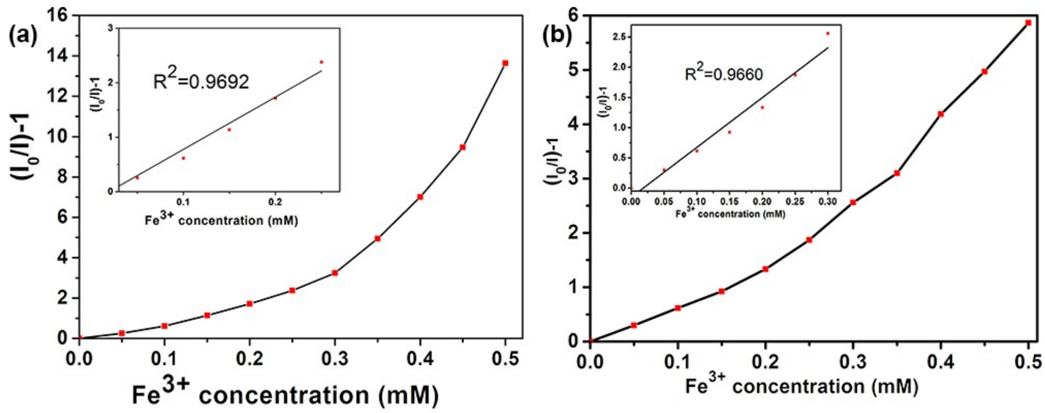

Fig. S7 S-V plot of **FJI-C8** suspended in DMF (a) 0.4 mg/mL, (b) 0.04 mg/mL upon incremental addition of $M(NO_3)_x$ (10 mM).

Table S3 Quenching effect coefficients (K_{sv}) of $M(NO_3)_x$ effect on the luminescence intensity of molecule incorporated **FJI-C8** suspension sample.

No.	$M(NO_3)_x$	K_{sv} (M^{-1})
1 [a]	$Fe(NO_3)_3$	8496
2	$Cu(NO_3)_2$	2055
3	$Co(NO_3)_2$	1242
4	$Cr(NO_3)_3$	1169
5	KNO_3	883
6	$Mg(NO_3)_2$	666
7 [b]	$Fe(NO_3)_3$	9590
8 [c]	$Fe(NO_3)_3$	8240

a the concentration of **FJI-C8** solution was 2mg/mL

b the concentration of **FJI-C8** solution was 0.4mg/mL

c the concentration of **FJI-C8** solution was 0.04mg/mL

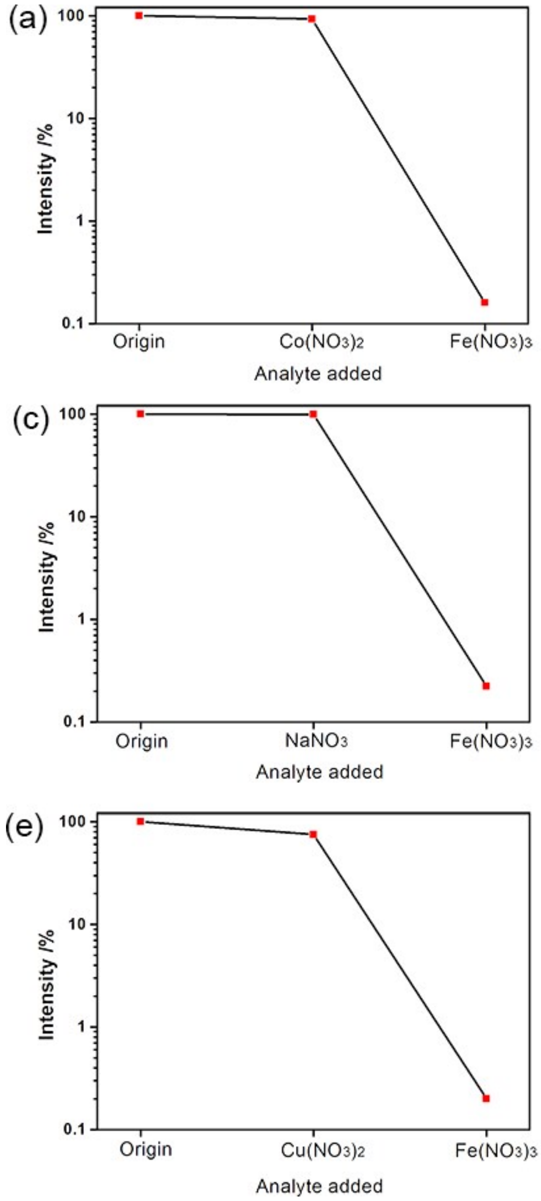

Fig. S8 Decrease in fluorescence intensity upon adding $M(NO_3)_x$ solution (1 mL stock suspension, 1 mL DMF, 10 μL $M(NO_3)_x$ (1 M), and 10 μL $Fe(NO_3)_3$ (1 M)).

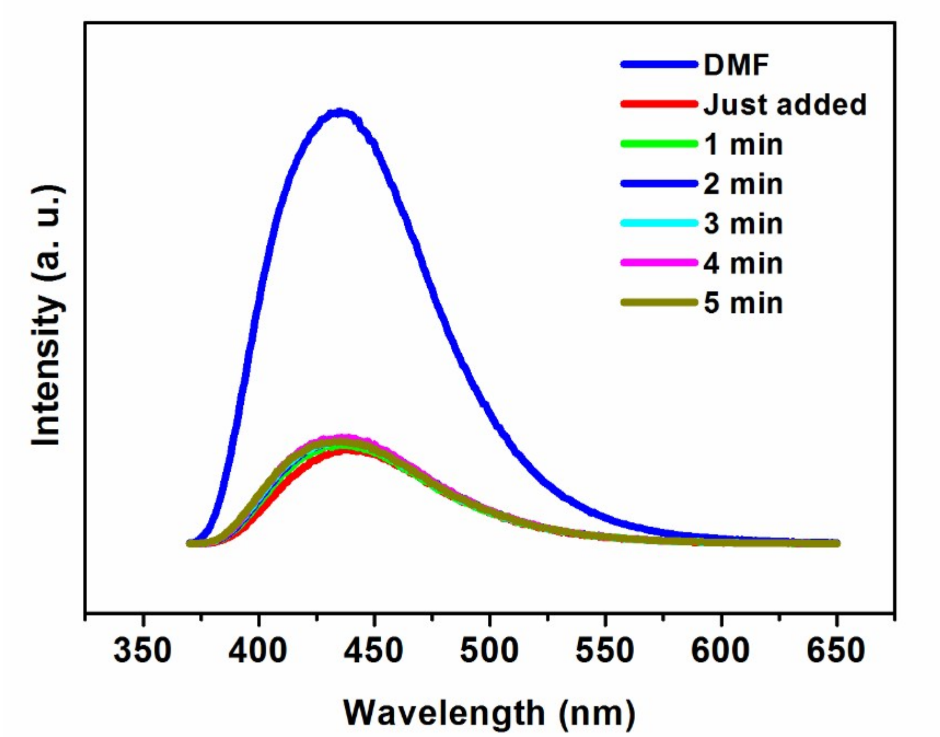

Fig. S9 Time-dependent fluorescence quenching detections of $Fe(NO_3)_3$ (1 mL stock suspension, 1 mL DMF, and 0.1 mL analyte solution (10 mM)).

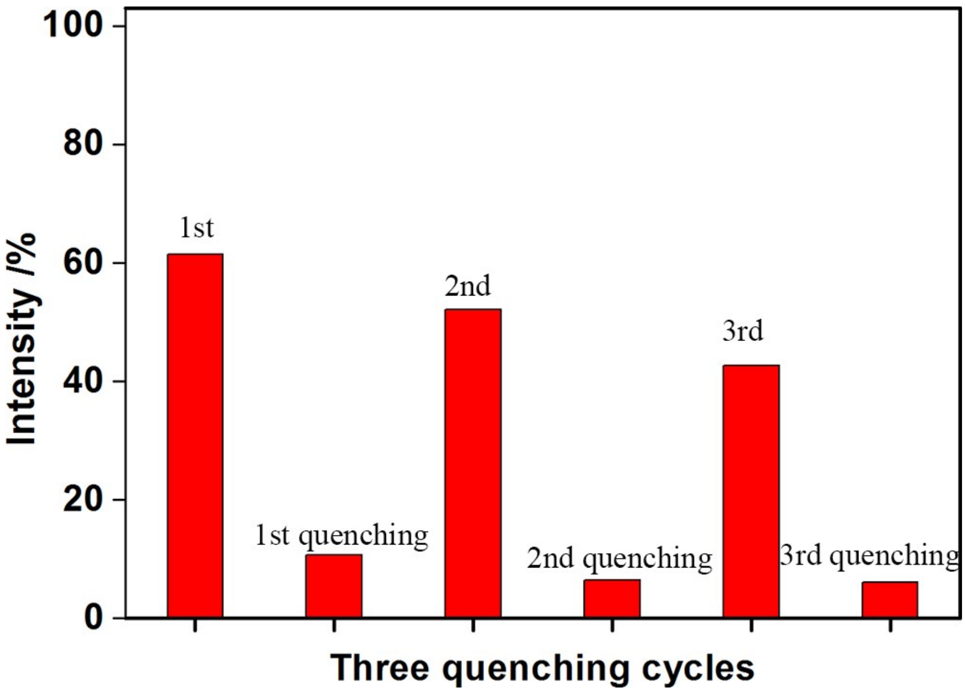

Fig. S10 Three quenching cycles of the **FJI-C8** dispersed in DMF with the addition of $Fe(NO_3)_3$ solution (1 mL stock suspension, 1 mL DMF, and 0.1 mL analyte solution (10 mM)).

Standard deviation and detection limit calculation

To calculate the standard deviation and detection limit of this detection method, **FJI-C8** with fine particles was made into a 2 mg/mL suspension. Then, $Fe(NO_3)_3$ solution (1 mM, 10-100 μL) was added into the suspension and the fluorescent intensities were recorded. Standard deviation (σ) was calculated from five blank tests of **FJI-C8** suspension and the detection limit was calculated via the formula: 3σ/m (m: the slope of the fitting line).

Table S4 Standard deviation calculation

Entry	Fluorescence intensity ($\times 10^6$)
Test 1	1.437
Test 2	1.502
Test 3	1.488
Test 4	1.514
Test 5	1.467
Standard deviation (σ)	0.0272

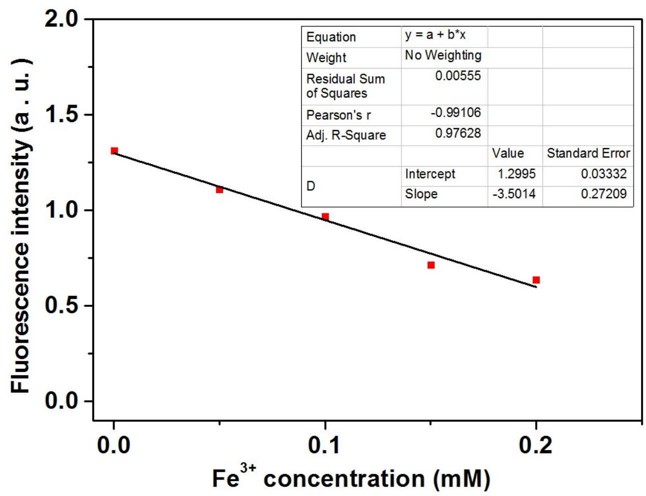

Fig. S11 Linear curve of fluorescence intensity of **FJI-C8** suspension upon incremental addition of Fe^{3+} (10 mM).

Table S5 Detection limit calculation for Fe^{3+}.

Slope (m)	3.50×10^6 mM^{-1}
Detection limit (3σ/m)	0.0233 mM

3. Ions detection with FJI-C8 solid

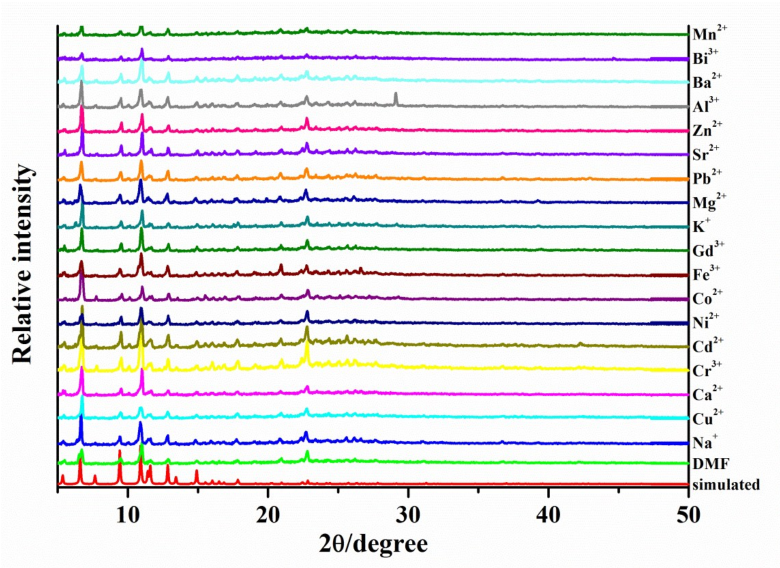

Fig. S12 PXRD of metal ion incorporated **FJI-C8** (metal ion stands for K^+, Hg^{2+}, Co^{2+}, Ba^{2+}, Na^+, Gd^{2+}, Zn^{2+}, Mg^{2+}, Cr^{3+}, Ni^{2+}, Ca^{2+}, Pb^{2+}, Al^{3+}, Sr^{2+}, Bi^{3+}, Mn^{2+}, Cu^{2+}, or Fe^{3+}).

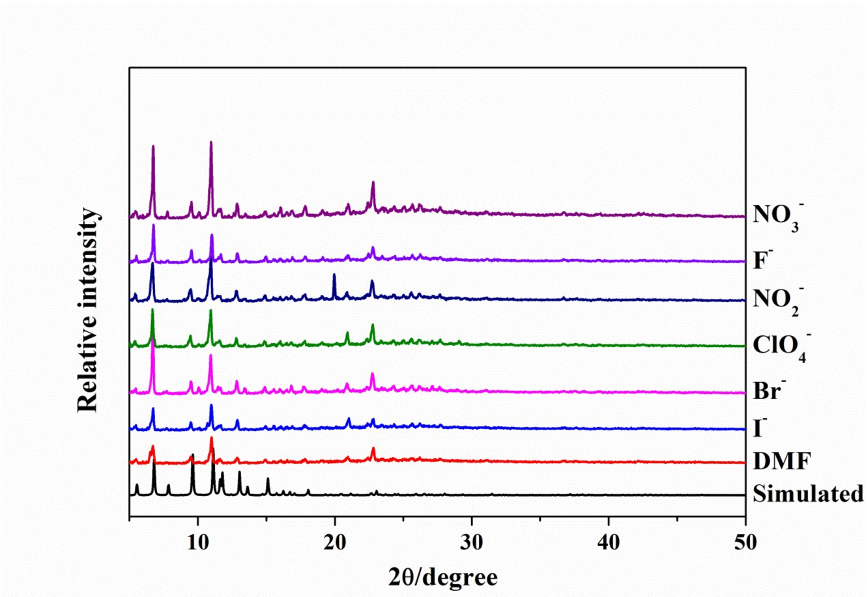

Fig. 13 The PXRD of anion incorporated **FJI-C8** (anion stands for F^-, Br^-, I^-, NO_2^-, NO_3^-, ClO_4^-).

Table S6 Quenching effect coefficients (K_{sv}) of different metal ions detected by **FJI-C8** solid sample.

No.	Metal ion	K_{sv}
1	K^{+}	7
2	Co^{2+}	18
3	Na^{+}	32
4	Gd^{2+}	44
5	Cd^{2+}	45
6	Zn^{2+}	47
7	Mg^{2+}	64
8	Cr^{3+}	72
9	Ni^{2+}	81
10	Ca^{2+}	82
11	Al^{3+}	87
12	Sr^{2+}	119
13	Bi^{3+}	121
14	Mn^{2+}	121
15	Cu^{2+}	143
16	Fe^{3+}	2188

Table S7 Quenching effect coefficients (K_{sv}) of different anions detected by **FJI-C8** solid sample.

No.	**Anions**	$\boldsymbol{K_{sv}}$
1	F^{-}	11
2	NO_3^{-}	32
3	ClO_4^{-}	46
4	NO_2^{-}	52
5	Br^{-}	63
6	I^{-}	88

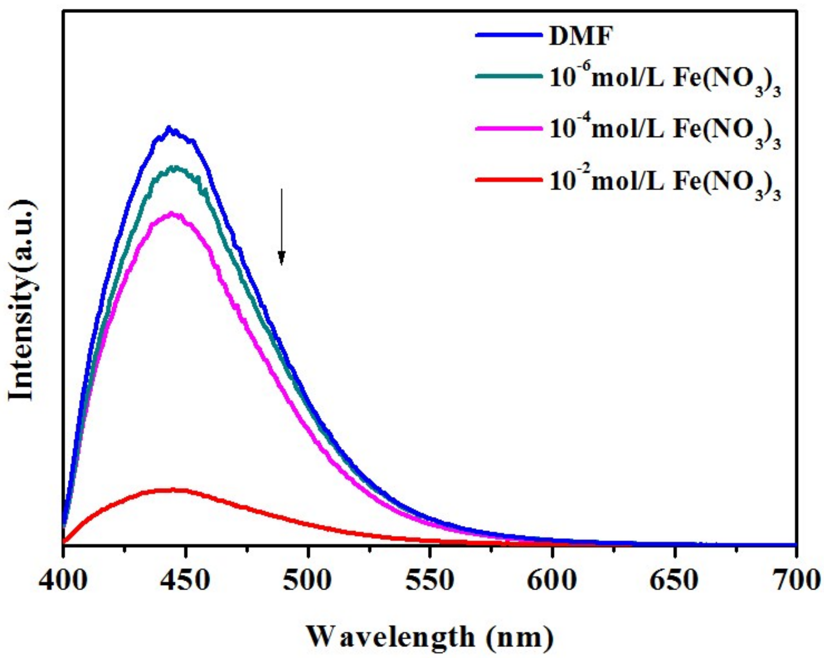

Fig. S14 The emission intensity of **FJI-C8** suspension after addition of $M(NO_3)_x$.

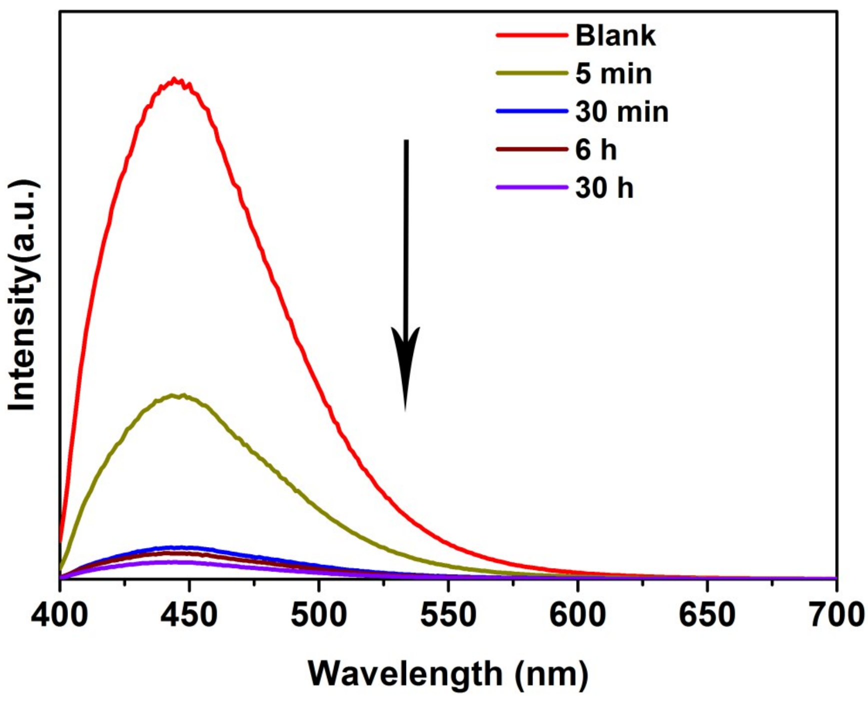

Fig. S15 Time-dependent fluorescence quenching detections of $Fe(NO_3)_3$ with **FJI-C8** solid after filtration.

4. Detection mechanisms

Table S8 Integral orbital overlap J (λ) values of $M(NO_3)_x$ absorption spectrum and **FJI-C8** emission spectrum.

No.	$M(NO_3)_x$	J (λ)
1	$Fe(NO_3)_3$	10.56
2	$Cu(NO_3)_2$	<0.1
3	$Co(NO_3)_2$	<0.1
4	$Cr(NO_3)_3$	<0.1
5	KNO_3	<0.1
6	$Mg(NO_3)_2$	<0.1

Table S9 Integral orbital overlap J (λ) values of $M(NO_3)_x$ absorption spectrum and **FJI-C8** excitation spectrum.

No.	$M(NO_3)_x$	J (λ)
1	$Fe(NO_3)_3$	37.53
2	$Cu(NO_3)_2$	4.79
3	$Co(NO_3)_2$	2.17
4	$Cr(NO_3)_3$	<0.1
5	KNO_3	<0.1
6	$Mg(NO_3)_2$	<0.1

TCSPC Study

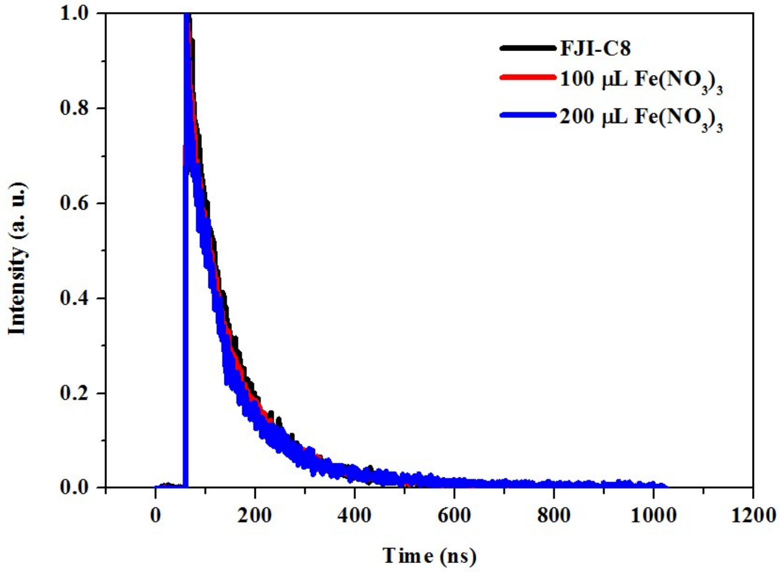

Fig. S16 Fluorescence lifetime decay profile of **FJI-C8** before and after adding of $Fe(NO_3)_3$.

Table S10 Fluorescence life time data for **FJI-C8** with $Fe(NO_3)_3$.

Adding amount	τ_1 [ns]	α_1	τ_2 [ns]	α_2	τ_{av} [ns]
0 µL	3.28	44.47	7.62	55.53	5.69
100 µL	3.34	47.25	8.17	52.75	5.89
200 µL	3.15	48.68	8.80	51.32	6.05

Table S11 Summary of the chemosensor suspension concentration for metal ions detection detection.

MOF	**Concentration of suspension**	**Sensitivity (mM)**	**Selectivity (M^{-1})**	**Ref.**
UMCM-1	0.2 mg/mL	--	--	1
UMCM-1-NH_2	0.2 mg/mL	--	--	1
La-MOF	0.25 mg/mL	--	13600	2
NNU-1	1.7 mg/mL	0.2	--	3
Eu_4L_3	1.5 mg/mL	--	2942	4
{[Tb(L)(DMA)]·(DMA)·(0.5H_2O)}	0.2 mg/mL	--	1913	5
[$(CH_3)_2NH_2$]·[Tb(bptc)]	0.8 mg/mL	0.1801	--	6
BUT-14	0.33 mg/mL	0.0038	2170	7
BUT-15	0.33 mg/mL	0.0003	16600	7
FJI-C8	**0.04 mg/mL**	**0.0233**	**8245**	**This work**

Ref.

1. Z. Xiang, C. Fang, S. Leng and D. Cao, *J. Mater. Chem. A*, 2014, **2**, 7662.
2. C. Zhang, Y. Yan, Q. Pan, L. Sun, H. He, Y. Liu, Z. Liang and J. Li, *Dalton Trans*, 2015, **44**, 13340-13346.
3. B. L. Hou, D. Tian, J. Liu, L. Z. Dong, S. L. Li, D. S. Li and Y. Q. Lan, *Inorg. Chem.*, 2016, **55**, 10580-10586.
4. W. Liu, X. Huang, C. Xu, C. Chen, L. Yang, W. Dou, W. Chen, H. Yang and W. Liu, *Chem. Eur. J.*, 2016, **22**, 18769-18776.
5. S. Pal and P. K. Bharadwaj, *Cryst. Growth Des.*, 2016, **16**, 5852-5858.
6. X. L. Zhao, D. Tian, Q. Gao, H. W. Sun, J. Xu and X. H. Bu, *Dalton Trans*, 2016, **45**, 1040-1046.
7. B. Wang, Q. Yang, C. Guo, Y. Sun, L. H. Xie and J. R. Li, *ACS Appl. Mater. Inter.*, 2017, **9**, 10286-10295.